



## Radiotracers for cardiac sympathetic innervation: Transport kinetics and binding affinities for the human norepinephrine transporter

David M. Raffel<sup>a,\*</sup>, Wei Chen<sup>a</sup>, Yong-Woon Jung<sup>a</sup>, Keun Sam Jang<sup>a</sup>, Guie Gu<sup>a</sup>, Nicholas V. Cozzi<sup>b</sup>

<sup>a</sup> Division of Nuclear Medicine, Department of Radiology, 2276 Medical Sciences 1 Building, University of Michigan Medical School, 1301 Catherine Street, SPC 5610, Ann Arbor, MI 48109, USA

<sup>b</sup> Neuropharmacology Laboratory, Department of Cell and Regenerative Biology, 2695 Medical Sciences Center, University of Wisconsin School of Medicine and Public Health, Madison, WI 53706, USA

### ARTICLE INFO

#### Article history:

Received 7 March 2012

Received in revised form 16 November 2012

Accepted 28 November 2012

#### Keywords:

Positron emission tomography

Hydroxyephedrine

Biogenic amines

Isolated rat heart

C6 glioma cells

### ABSTRACT

**Introduction:** Most radiotracers for imaging of cardiac sympathetic innervation are substrates of the norepinephrine transporter (NET). The goal of this study was to characterize the NET transport kinetics and binding affinities of several sympathetic nerve radiotracers, including [<sup>11</sup>C]-(-)-*meta*-hydroxyephedrine, [<sup>11</sup>C]-(-)-epinephrine, and a series of [<sup>11</sup>C]-labeled phenethylguanidines under development in our laboratory. For comparison, the NET transport kinetics and binding affinities of some [<sup>3</sup>H]-labeled biogenic amines were also determined.

**Methods:** Transport kinetics studies were performed using rat C6 glioma cells stably transfected with the human norepinephrine transporter (C6-hNET cells). For each radiolabeled NET substrate, saturation transport assays with C6-hNET cells measured the Michaelis–Menten transport constants  $K_m$  and  $V_{max}$  for NET transport. Competitive inhibition binding assays with homogenized C6-hNET cells and [<sup>3</sup>H]mazindol provided estimates of binding affinities ( $K_i$ ) for NET.

**Results:**  $K_m$ ,  $V_{max}$  and  $K_i$  values were determined for each NET substrate with a high degree of reproducibility. Interestingly, C6-hNET transport rates for ‘tracer concentrations’ of substrate, given by the ratio  $V_{max}/K_m$ , were found to be highly correlated with neuronal transport rates measured previously in isolated rat hearts ( $r^2 = 0.96$ ). This suggests that the transport constants  $K_m$  and  $V_{max}$  measured using the C6-hNET cells accurately reflect in vivo transport kinetics.

**Conclusion:** The results of these studies show how structural changes in NET substrates influence NET binding and transport constants, providing valuable insights that can be used in the design of new tracers with more optimal kinetics for quantifying regional sympathetic nerve density.

© 2013 Elsevier Inc. All rights reserved.

### 1. Introduction

[<sup>11</sup>C]-(-)-*meta*-Hydroxyephedrine (HED) and [<sup>11</sup>C]-(-)-epinephrine (EPI) are two of the current generation of positron emission tomography (PET) radiotracers used to assess the integrity of cardiac sympathetic nerve terminals [1]. As structural analogs of the endogenous neurotransmitter norepinephrine, HED and EPI are transported into cardiac sympathetic nerve varicosities by norepinephrine transporters (NET) localized in the outer membranes of terminal sympathetic nerve axons [2,3]. Once inside neurons, they are transported into norepinephrine storage vesicles by the second isoform of the vesicular monoamine transporter (VMAT2).

While HED and EPI both accumulate in cardiac sympathetic neurons by the same transport pathways as norepinephrine, there

are differences in the kinetics of their neuronal uptake and retention. For example, kinetic studies in isolated rat hearts have shown that HED is transported into neurons by NET at a rate that is more than four times faster than EPI (2.66 vs. 0.60 ml/min/g wet, respectively) [2,3]. Also, studies have shown that HED is lipophilic enough ( $\log P = 0.3$ ) to diffuse fairly quickly out of vesicles and neurons [2]. After leaking from neurons, HED is usually taken back up by neurons, setting up a dynamic recycling of HED molecules during PET imaging. On the other hand, EPI is a very polar catecholamine ( $\log P = -1.30$ ) that remains tightly sequestered inside storage vesicles [3]. Isolated rat heart studies of the kinetics and retention mechanisms of cardiac sympathetic nerve radiotracers have provided invaluable insights into differences in the neuronal uptake and storage of these imaging agents [4]. Such insights are critical to interpreting changes observed in the kinetics and myocardial retention of a specific tracer in clinical PET studies of heart diseases [1].

In this study, we sought to better characterize the kinetic properties of HED and EPI by measuring their Michaelis–Menten transport constants  $K_m$  and  $V_{max}$  for NET transport. To accomplish this

\* Corresponding author. Tel.: +1 734 936 0725; fax: +1 734 764 0288.  
E-mail address: [raffel@umich.edu](mailto:raffel@umich.edu) (D.M. Raffel).

goal, we performed transport kinetics assays using a rat C6 glioma cell line stably transfected with the cloned human NET (C6-hNET cells), a gift from Dr. Amy Eshleman, Oregon Health Sciences University, Portland, OR. For comparison, we also measured  $K_m$  and  $V_{max}$  values for the biogenic amines norepinephrine and dopamine. In addition, we performed competitive inhibition binding assays using membranes from homogenized C6-hNET cells to determine the binding affinities ( $K_i$ ) of each compound for hNET.

$K_m$ ,  $V_{max}$  and  $K_i$  values were also measured for five [ $^{11}C$ ]-labeled phenethylguanidines. Our laboratory is currently investigating radiolabeled phenethylguanidines in an effort to develop a new PET sympathetic nerve imaging agent with more optimal kinetics for quantifying regional nerve density using tracer kinetic analyses [5]. Assessment of the kinetic profiles of these new compounds not only provides valuable structure–activity relation data but also allows comparisons with the existing radiotracers and biogenic amines.

## 2. Materials and methods

### 2.1. Radiochemistry

[ $^{11}C$ ]-(-)-*meta*-Hydroxyephedrine (HED) and [ $^{11}C$ ]-(-)-epinephrine (EPI) were prepared using previously published methods [6,7]. The five different [ $^{11}C$ ]-labeled phenethylguanidines studied were synthesized using methods previously reported [5].

### 2.2. Chemicals

[4'- $^3H$ ]Mazindol (NET-816; specific activity 24.5 Ci/mmol), levo-[ring-2,5,6- $^3H$ ]norepinephrine (NET-678; specific activity 74.9 Ci/mmol) and 3,4-[ring-2,5,6- $^3H$ ]dihydroxyphenylethylamine (NET-673; specific activity 59.3 Ci/mmol) were purchased from Perkin Elmer/New England Nuclear (Boston, MA, USA). Desipramine hydrochloride, (-)-norepinephrine hydrochloride, (-)-epinephrine bitartrate, dopamine hydrochloride, (-)-*erythro*-metaraminol bitartrate, tyramine and assay buffer reagents were purchased from Sigma-Aldrich Corp. (St. Louis, MO). *meta*-Tyramine was purchased from Trans World Chemicals, Rockville, MD, USA). (-)-*erythro*-*meta*-Hydroxyephedrine hydrochloride, (-)-*meta*-octopamine, (-)-*N*-guanyl-*meta*-octopamine, *para*-fluoro-*meta*-hydroxyphenethylamine, *para*-fluoro-*meta*-hydroxyphenethylguanidine, *ortho*-fluoro-*meta*-hydroxyphenethylamine, and *ortho*-fluoro-*meta*-hydroxyphenethylguanidine were prepared in our laboratory, as previously described [5].

### 2.3. C6-hNET cells

Rat C6 glial tumor cells stably transfected with the human norepinephrine transporter (C6-hNET cells) were a gift from Dr. Amy Eshleman, Oregon Health Sciences University, Portland, OR. Cells were maintained in a humidified atmosphere (5% CO<sub>2</sub> in air) in selective culture medium: Dulbecco's Modified Eagle's Medium (DMEM) containing 10% fetal bovine serum, 200 mM L-glutamine and antibiotics (100 U/ml penicillin, 100 µg/ml streptomycin, 200 µg/ml Geneticin).

### 2.4. Transport kinetics assays

C6-hNET cells were grown to confluence in a 75 cm<sup>2</sup> tissue culture flask. Medium was removed, the cells washed with 5 ml of phosphate buffered saline (pH = 7.4), then treated with 2 ml of trypsin/EDTA and split into two 24-well plates. For the split, cells were diluted with enough medium so that each well contained 1.5–1.7 × 10<sup>5</sup> cells in 1 ml of the selective culture medium. Cells were grown overnight (21–24 h) to confluence. For the transport assay, Krebs–Ringer–HEPES (KRH) buffer was used, containing (mM): NaCl (124), KCl (2.9), MgSO<sub>4</sub> (1.3), KH<sub>2</sub>PO<sub>4</sub> (1.2), CaCl<sub>2</sub> (2.4), D-glucose (5.2), HEPES (25), sodium ascorbate (0.1)

and pargyline (0.1), pH = 7.4. Prior to the assay, cells were rinsed with 3 × 1 ml KRH buffer at 37 °C. In the first 24-well plate, which was used to determine total (specific + nonspecific) tracer uptake, 400 µl of 37 °C KRH buffer was added to each well. In the second plate, which was used to measure nonspecific uptake, 400 µl of KRH buffer containing 50 µM of the potent NET inhibitor desipramine (DMI) was added to each well (final DMI concentration 10 µM). Plates were preincubated for 10 min at 37 °C in a shaking water bath, then 100 µl of KRH buffer containing a mixture of radiolabeled NET substrate and its corresponding unlabeled substrate at a known concentration was added to initiate uptake. Triplicate determinations of uptake were made for each substrate concentration in the assay. After incubation for 5 min at 37 °C, incubation buffer was rapidly removed and the cells were washed with 4 × 1 ml ice-cold KRH buffer. The process of adding substrate, removing substrate and washing was staggered in time for the 7 different substrate concentrations to minimize the time necessary to complete the assay. This was essential for [ $^{11}C$ ]-labeled substrates due to the short half-life of carbon-11 (20.4 min). Once all incubations were completed, cells were solubilized by adding 300 µl 1% sodium dodecyl sulfate (SDS) to each well and shaking for 15 min. For [ $^3H$ ]-labeled substrates, well contents were transferred to 20 ml scintillation vials, another 200 µl 1% SDS was added to each well as a rinse and transferred to the appropriate vial. For each substrate concentration, triplicate 100 µl samples of the buffer containing radiolabeled substrate were placed in scintillation vials for measurement of substrate concentration. After adding 10 ml scintillation cocktail (UniverSol ES, MP Biomedicals, Solon, OH, USA) the vials were counted in a liquid scintillation counter to determine the activity in each vial. For [ $^{11}C$ ]-labeled substrates, the solubilized well contents were counted in a gamma counter to measure carbon-11 activity. A set of carbon-11 standards was prepared by adding a small amount of the radiotracer to 1.0 ml of water and performing serial two-fold dilutions to make a set of ten 0.5 ml standards over a range of activities. The activity of the most concentrated standard was determined in a dose-calibrator. These standards were counted with the assay samples and used to correct measured counts-per-minute (cpm) into activity values. All carbon-11 measurements were decay corrected. A total of ~74 MBq (2 mCi) of [ $^{11}C$ ]-labeled substrate was needed to obtain good counting statistics and the entire experiment, including counting of samples, was completed in less than 1 h. For each radiolabeled NET substrate studied,  $n = 4$  or 5 assays were performed.

### 2.5. C6-hNET membrane preparation for binding assays

One 75 cm<sup>2</sup> tissue culture flask of confluent C6-hNET cells was split 1:3 into 150 mm culture dishes and grown to confluence (2 d). Each dish was split 1:8 into 150 mm culture dishes and again grown to confluence (2 d). Medium was removed and cells washed once with 3 × 6 ml phosphate-buffered saline (PBS) pH 7.4, then washed with 2 × 6 ml of homogenization buffer A (HB-A) containing (mM): NaCl (150), HEPES (10), EDTA (1.0), MgCl<sub>2</sub> (0.1), pH = 7.4. Cells were scraped from the dish under 3 ml of HB-A, collected, and the dish rinsed again with 2 ml of HB-A. Collected cells from eight dishes (enough for one assay) were centrifuged at 100 × g for 5 min at 4 °C. The pellet was resuspended in 2 ml of homogenization buffer B (HB-B; 1 tablet of Complete™ Mini protease inhibitor cocktail [Roche, Indianapolis, IN, USA] dissolved in 100 ml of HB-A). The cells were homogenized by hand in a 7 ml Dounce homogenizer using ~30 up and down strokes. A homogenate sample was inspected using microscopy to ensure that >95% of the cells were broken. HB-B was added to bring the volume to 6 ml and the mixture centrifuged at 500 × g for 10 min at 4 °C. The supernatant was centrifuged at 100,000 × g for 30 min at 4 °C. The pellet was resuspended in 6 ml of assay buffer (50 mM Tris, 120 mM NaCl, 5 mM KCl, pH = 7.4) and centrifuged again (100,000 × g, 30 min). The final pellet was resuspended in 5 ml of assay buffer and stored at –80 °C.

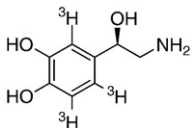
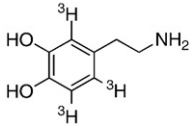
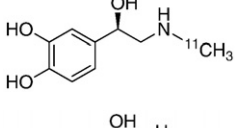
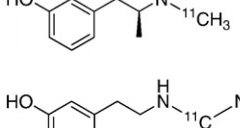
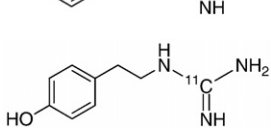
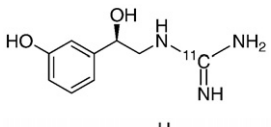
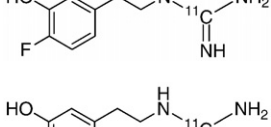
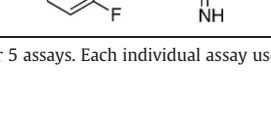

## 2.6. Binding assays

For all assays, protein concentrations of the C6-hNET membrane preparations were measured with the Lowry spectrophotometric method [8], using bovine serum albumin for standards. Competitive inhibition studies with the NET radioligand [<sup>3</sup>H]mazindol were performed to measure NET binding affinities ( $K_i$ ) for each substrate studied in the transport assays. Assays were performed as previously described for rat heart homogenates [9], except that the assay used 100  $\mu$ l of the C6-hNET membrane preparation (70–100  $\mu$ g protein). DMI was again used to define nonspecific binding. Quadruplicate determinations of specific binding were made at 10 different inhibitor concentrations, and the data normalized to control levels of specific binding to express the data as “% specific binding”. Saturation binding assays were also performed with C6-hNET cell membranes to measure the equilibrium dissociation constant  $K_D$  of [<sup>3</sup>H]mazindol for NET in this preparation, again using methods previously reported for rat heart homogenates [9]. Membranes were incubated at eight different [<sup>3</sup>H]mazindol concentrations (range 0.25–25 nM) and triplicate determinations of specific [<sup>3</sup>H]mazindol binding were made at each concentration.

## 2.7. Data analysis and statistics

Transport or binding parameters were determined by fitting the specific uptake or specific binding data from transport or binding assays to the appropriate equation using nonlinear regression (GraphPad Prism™, GraphPad Software, San Diego, CA). For transport assays, a one-carrier transport model with initial velocity of transport  $V_{init} = [S]V_{max}/([S] + K_m)$ , where [S] = substrate concentration, was used to estimate the transport parameters  $K_m$  (half-saturation concentration;  $\mu$ M) and  $V_{max}$  (maximum velocity of transport; pmol/min/mg protein). For saturation binding assays with C6-hNET membranes, the specific binding versus [<sup>3</sup>H]mazindol concentration data were fitted to a one-site binding model to estimate  $K_D$  (nM) and  $B_{max}$  (fmol/mg protein). For competitive binding assays, the percentage specific binding versus inhibitor concentration data were fitted to a one-site competition model.  $K_i$  values were calculated from estimated  $IC_{50}$  values using the Cheng-Prusoff correction,  $K_i = IC_{50}/(1 + L^*/K_D)$ , where  $L^*$  is the [<sup>3</sup>H]mazindol concentration used and  $K_D$  was set to the mean value from control saturation assays (1.20 nM).

**Table 1**  
Binding affinities ( $K_i$ ) and Michaelis–Menten transport parameters ( $K_m$ ,  $V_{max}$ ) for the cloned human norepinephrine transporter stably expressed in rat C6-glia cells (C6-hNET cells).

NET Substrate	Acronym	Structure	$K_i$ ( $\mu$ M)	$K_m$ ( $\mu$ M)	$V_{max}$ (pmol/min/mg protein)	$V_{max}/K_m$ ( $\mu$ l/min/mg protein)
[ <sup>3</sup> H](–)-norepinephrine	NE		63.9 $\pm$ 2.3	0.28 $\pm$ 0.03	5.83 $\pm$ 0.49	21.3 $\pm$ 2.4
[ <sup>3</sup> H]dopamine	DA		8.1 $\pm$ 0.5	0.24 $\pm$ 0.04	2.91 $\pm$ 0.47	12.2 $\pm$ 1.8
[ <sup>11</sup> C](–)-epinephrine	EPI		68.4 $\pm$ 7.6	3.16 $\pm$ 0.78	6.09 $\pm$ 1.04	2.0 $\pm$ 0.2
[ <sup>11</sup> C](–)-meta-hydroxyephedrine	HED		43.2 $\pm$ 1.8	0.48 $\pm$ 0.08	5.43 $\pm$ 0.71	11.4 $\pm$ 1.3
[ <sup>11</sup> C]meta-hydroxyphenethylguanidine	MHPG		4.9 $\pm$ 0.5	0.73 $\pm$ 0.20	7.83 $\pm$ 1.73	11.2 $\pm$ 2.8
[ <sup>11</sup> C]para-hydroxyphenethylguanidine	PHPG		1.9 $\pm$ 0.2	0.52 $\pm$ 0.06	3.31 $\pm$ 0.40	6.4 $\pm$ 1.1
(–)-N-[ <sup>11</sup> C]guanylmeta-octopamine	GMO		20.3 $\pm$ 2.5	4.43 $\pm$ 0.31	5.57 $\pm$ 0.30	1.3 $\pm$ 0.1
[ <sup>11</sup> C]4-fluoro-meta-hydroxyphenethylguanidine	4F-MHPG		5.6 $\pm$ 0.5	2.57 $\pm$ 0.35	7.46 $\pm$ 0.64	3.0 $\pm$ 0.5
[ <sup>11</sup> C]6-fluoro-meta-hydroxyphenethylguanidine	6F-MHPG		17.7 $\pm$ 0.5	2.86 $\pm$ 0.43	4.06 $\pm$ 0.66	1.4 $\pm$ 0.3

Values are means  $\pm$  standard deviations for  $n = 4$  or 5 assays. Each individual assay used triplicate determinations of uptake at each concentration of substrate.

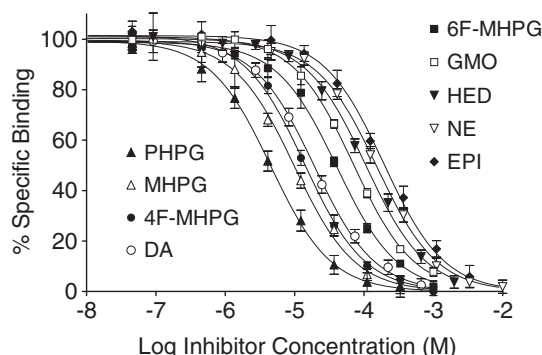


**Fig. 1.** Competitive inhibition of [ $^3\text{H}$ ]mazindol binding to hNET in homogenized C6-hNET cell membrane preparations. Values plotted are means  $\pm$  SEM of quadruplicate determinations of specific binding at each time point. Acronyms for each compound, along with all competitive inhibition assay results, are given in Table 1.

### 3. Results

#### 3.1. Binding assays

Saturation binding assays with [ $^3\text{H}$ ]mazindol and different batches of C6-hNET membranes were performed to determine the equilibrium dissociation constant  $K_D$  for [ $^3\text{H}$ ]mazindol binding to NET in the C6-hNET cell membrane preparations. Mean binding parameters were  $K_D = 1.20 \pm 0.17$  nM and  $B_{\text{max}} = 457 \pm 31$  fmol/mg protein ( $n = 4$ ). In competitive inhibition studies of [ $^3\text{H}$ ]mazindol binding to C6-hNET cell membranes, the data from all studies were well-described by a one-site competition model.  $K_I$  values of the substrates studied ranged from  $1.9 \pm 0.2$   $\mu\text{M}$  for *para*-hydroxyphenethylguanidine to  $68.4 \pm 7.6$   $\mu\text{M}$  for (–)-epinephrine (Table 1; Fig. 1).

#### 3.2. Transport kinetics assays

The transport parameters  $K_m$  and  $V_{\text{max}}$  measured for each NET substrate are summarized in Table 1. Ratios of  $V_{\text{max}}/K_m$ , which reflect NET transport rates at tracer-level substrate concentrations (i.e.,  $[S] \ll K_m$ ), are also given in Table 1. Representative transport assay data are shown in Fig. 2. In all cases, the specific uptake data were well-described by a one-site transport model. [ $^3\text{H}$ ](–)-Norepinephrine and [ $^3\text{H}$ ]dopamine had the lowest  $K_m$  values while [ $^{11}\text{C}$ ]meta-hydroxyphenethylguanidine (MHPG) and [ $^{11}\text{C}$ ]4-fluoro-*meta*-hydroxyphenethylguanidine (4F-MHPG) had the highest  $V_{\text{max}}$  values.  $V_{\text{max}}/K_m$  ratios ranged from  $1.3 \pm 0.1$   $\mu\text{l}/\text{min}/\text{mg}$  protein for (–)-*N*-[ $^{11}\text{C}$ ]guanyl-*meta*-octopamine (GMO) to  $21.3 \pm 2.4$   $\mu\text{l}/\text{min}/\text{mg}$  protein for [ $^3\text{H}$ ](–)-norepinephrine. No correlation was found between the

measured  $K_I$ ,  $K_m$  and  $V_{\text{max}}$  values, suggesting that each constant is independently influenced by structural changes of NET substrates, at least for the cloned human NET expressed in this cell line. However, C6-hNET transport rates for tracer-level concentrations of substrate ( $[S] \ll K_m$ ), given by the  $V_{\text{max}}/K_m$  ratios, were found to be highly correlated with NET-mediated uptake rates into sympathetic neurons previously measured in isolated perfused rat hearts ( $r^2 = 0.96$ , Fig. 3) [5,10,11]. This result strongly suggests that the transport parameters measured in vitro using C6-hNET cells accurately reflect in vivo NET transport kinetics.

### 4. Discussion

In PET studies of cardiac sympathetic innervation with high specific activity  $^{11}\text{C}$ -labeled NET substrates such as [ $^{11}\text{C}$ ](–)-*meta*-hydroxyephedrine (HED) and [ $^{11}\text{C}$ ](–)-epinephrine (EPI), tracer-level concentrations of the substrates are used. The substrate concentration  $[S]$  outside the neuronal membrane is much lower than the half-saturation transport concentration  $K_m$ , so that  $[S] \ll K_m$ . In this case, the classic Michaelis–Menten equation describing the initial velocity of transport,  $V_{\text{init}} = [S]V_{\text{max}}/([S] + K_m)$ , simplifies to the equation  $V_{\text{init}} = (V_{\text{max}}/K_m)[S]$ . Thus it is the ratio of a substrate's Michaelis–Menten transport constants  $V_{\text{max}}$  and  $K_m$  that determines its in vivo neuronal uptake rate. The ratio  $V_{\text{max}}/K_m$  for a radiolabeled NET substrate is effectively a ‘neuronal NET transport rate constant’ for the substrate – a high value of the ratio indicates a rapid neuronal NET transport rate for tracer concentrations of the substrate, and a low value implies a slower NET transport rate.

The isolated perfused rat heart model has been used extensively to characterize the neuronal and extraneuronal uptake of biogenic amines. In pioneering studies, Iversen used this model to make some of the first measurements of norepinephrine transport kinetics in the heart [12]. Iversen coined the terms ‘uptake<sub>1</sub>’ for neuronal uptake by NET and ‘uptake<sub>2</sub>’ for extraneuronal uptake into rat heart myocytes [13]. By measuring the accumulation of [ $^3\text{H}$ ](–)-norepinephrine in hearts perfused with a range of total (–)-norepinephrine concentrations, Iversen estimated transport constants  $K_m = 0.27$   $\mu\text{M}$  and  $V_{\text{max}} = 1.18 \pm 0.12$  nmol/min/g wet for NET transport of norepinephrine [14]. Using these values to calculate the ratio  $V_{\text{max}}/K_m$ , a neuronal transport rate constant of  $4.37 \pm 0.44$  ml/min/g wet is obtained for norepinephrine (Table 2). Using similar methods, Hellmann et al. [11] measured  $K_m$  and  $V_{\text{max}}$  values for [ $^3\text{H}$ ]dopamine (Table 2).

More recently, the isolated rat heart has proven to be a valuable tool for studying the kinetics and neuronal retention mechanisms of radiotracers designed for noninvasive assessments of cardiac innervation using scintigraphic imaging. Kinetic studies of the neuronal uptake rates of sympathetic nerve radiotracers use a constant infusion

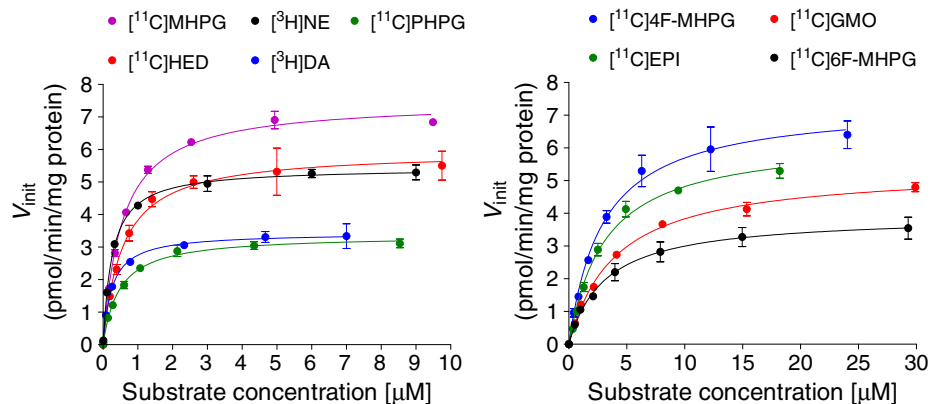


**Fig. 2.** Representative transport kinetics assays using intact C6-hNET cells. Compounds with low  $K_m$  values are shown in the left panel, those with higher  $K_m$  values are shown in the right panel. Values plotted are means  $\pm$  SEM of triplicate determinations of specific uptake at each concentration of NET substrate. Each individual assay shown was repeated  $n = 4$  or 5 times, with the  $K_m$  and  $V_{\text{max}}$  values estimated from each assay averaged together, as reported in Table 1.

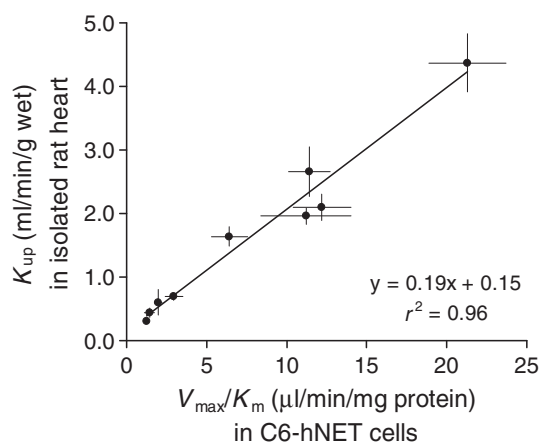


**Fig. 3.** For all radiolabeled NET substrates studied, the correlation between neuronal uptake rates in isolated rat hearts ( $K_{up}$ ; ml/min/g wet) and the corresponding ratio of Michaelis–Menten transport constants,  $V_{max}/K_m$ , determined *in vitro* using C6-hNET cells. Values plotted are means  $\pm$  SD ( $n=4$  or 5 each). For the C6-hNET transport studies, each of the  $n=4$  or 5 assays was performed using triplicate determinations of specific uptake at each concentration of substrate.

of tracer-level concentrations of the NET substrate to directly measure the ratio of the transport parameters,  $V_{max}/K_m$ . For example, the transport rate constant  $K_{up}=V_{max}/K_m$  was measured to be  $0.60 \pm 0.20$  ml/min/g wet for EPI [3], and  $2.66 \pm 0.39$  ml/min/g wet for HED [2] (Table 2). Iversen's approach to measuring NET transport kinetics has successfully been applied to [ $^{131}$ I]metaibenzylguanidine (MIBG) [15] and [ $^{76}$ Br]bromobenzylguanidine (MBBG) [16], which exhibit similar kinetic properties (Table 2). While it is possible to determine the NET transport constants in this way, such studies are challenging and time consuming to perform, requiring a large number of perfusion studies to yield estimates of  $K_m$  and  $V_{max}$ .

A goal of this study was to determine if the transport parameters  $K_m$  and  $V_{max}$  for NET substrates could be measured more efficiently using *in vitro* cell-based methods. Rat C6 glioma cells do not natively express monoamine transporters, including NET [17], the dopamine transporter (DAT) [18] or the serotonin transporter (SERT) [19]. Stable expression of the cloned human monoamine transporters in C6 glioma cells (C6-hNET, C6-hDAT and C6-hSERT cells) [18] offers a convenient *in vitro* system for performing structure–activity relationship studies of transporter substrates or inhibitors. For example, the C6-hNET cell line was previously used to study the stereoselective competitive inhibition of [ $^3$ H]-(-)-norepinephrine transport by the four stereoisomers of *meta*-hydroxyephedrine [20]. In the present work, each individual transport assay with a radiolabeled NET substrate using C6-hNET cells yielded estimates of  $K_m$  and  $V_{max}$ .

Compared to the more time-consuming studies in isolated rat hearts needed to obtain such estimates, the use of a transfected cell line greatly facilitates performance of structure–activity relation studies.

Neuronal transport of an NET substrate starts with the initial binding of the substrate to the transporter, with an association rate constant  $k_{on}$  and dissociation constant  $k_{off}$ , characterized by an equilibrium dissociation constant  $K_D=k_{off}/k_{on}$ .  $K_m$  and  $V_{max}$  values depend in a complex manner not only on the values of  $k_{on}$  and  $k_{off}$ , but also on rate constants that describe the rates at which the loaded transporter translocates the substrate through the neuronal membrane, the substrate is unloaded into the neuronal axoplasm, and the unloaded transporter reconfigures itself to again bind substrate outside the neuronal membrane [21]. Hence as part of this structure–activity study, binding affinities ( $K_i$ ) for NET were also assessed using membranes prepared from homogenized C6-hNET cells and the high affinity NET radioligand [ $^3$ H]mazindol in competitive inhibition assays.

For the biogenic amines dopamine (DA), (-)-norepinephrine (NE) and (-)-epinephrine (EPI), the estimated equilibrium dissociation constants ( $K_i$ ) followed the rank order  $DA < NE < EPI$ . This order is consistent with  $K_i$  values previously determined using rat heart homogenates under identical assay conditions [9]. However, absolute  $K_i$  values were 1.3 to 1.9 times higher in the C6-hNET membrane preparation than in the rat heart membranes. Similarly, the  $K_i$  of (-)-*meta*-hydroxyephedrine (HED) was 2.0 times higher in C6-hNET membranes than in rat heart membranes. These differences in measured  $K_i$  values between the two preparations could be due to true differences in substrate affinities between rat NET (rNET) and human NET (hNET). Alternatively, the differences may be because hNET cells expressed in rat C6 glioma cells are lacking some membrane-bound cofactors that are present for the rNET in their native cardiac membranes, resulting in lower measured binding affinities. All of the phenethylguanidine structures studied had higher binding affinities for hNET than the endogenous neurotransmitter norepinephrine and a few had binding affinities higher than dopamine.

Estimates of  $K_m$  and  $V_{max}$  from transport kinetics assays with intact C6-hNET cells and radiolabeled NET substrates were highly reproducible (Table 1). These data provide insights into how specific structural changes of NET substrates influence their transport kinetics by hNET. For example, the biogenic amine DA had the lowest  $K_m$  value of all compounds studied and an intermediate  $V_{max}$  value. Addition of a  $\beta$ -hydroxyl group to DA to form NE causes a slight increase in  $K_m$ , but increases  $V_{max}$  two-fold. Thus the tracer-level NET transport constant  $V_{max}/K_m$  is  $\sim 1.7$  times higher for NE than for DA. Addition of an *N*-methyl group to NE to form EPI leads to an 11-fold increase in  $K_m$  but does not significantly change  $V_{max}$ . In this case, the large increase in  $K_m$  for EPI causes  $V_{max}/K_m$  to be  $\sim 11$  times higher for NE than for EPI.

**Table 2**

Kinetics parameters for NET transport of various NET substrates as determined previously in isolated rat heart models.

NET Substrate	Acronym	$K_m$ ( $\mu$ M)	$V_{max}$ (nmol/min/g wet)	$V_{max}/K_m$ ratio (ml/min/g wet)	$K_{up}=V_{max}/K_m$ (ml/min/g wet)	Reference
[ $^3$ H]-(-)-norepinephrine	NE	0.27	$1.18 \pm 0.12$	$4.37 \pm 0.44$	—	Iversen [14]
[ $^3$ H]dopamine	DA	0.69	1.45	2.10	—	Hellmann et al. [11]
[ $^{11}$ C]-(-)-epinephrine	EPI	—	—	—	$0.60 \pm 0.20$	Nguyen et al. [3]
[ $^{11}$ C]-(-)- <i>meta</i> -hydroxyephedrine	HED	—	—	—	$2.66 \pm 0.39$	DeGrado et al. [2]
[ $^{11}$ C] <i>meta</i> -hydroxyphenethylguanidine	MHPG	—	—	—	$1.96 \pm 0.13$	Raffel et al. [5]
[ $^{11}$ C] <i>para</i> -hydroxyphenethylguanidine	PHPG	—	—	—	$1.64 \pm 0.15$	"
(-)- <i>N</i> -[ $^{11}$ C]guanyl- <i>meta</i> -octopamine	GMO	—	—	—	$0.30 \pm 0.02$	"
[ $^{11}$ C]4-fluoro- <i>meta</i> -hydroxyphenethylguanidine	4F-MHPG	—	—	—	$0.72 \pm 0.05$	"
[ $^{11}$ C]6-fluoro- <i>meta</i> -hydroxyphenethylguanidine	6F-MHPG	—	—	—	$0.49 \pm 0.07$	"
[ $^{131}$ I]metaiodobenzylguanidine	MIBG	0.052	0.23	4.4	$3.6 \pm 0.2$	DeGrado et al. [15]
[ $^{76}$ Br]- <i>meta</i> -bromobenzylguanidine	MBBG	$0.11 \pm 0.03$	$0.33 \pm 0.10$	$3.0 \pm 1.2$	$3.6 \pm 0.3$	Raffel et al. [16]

Values with  $\pm$  sign are mean  $\pm$  standard deviation.  $V_{max}/K_m$  ratios are the ratio of  $V_{max}$  and  $K_m$  estimates. Measured values of  $K_{up}$  (ml/min/g wet) are equal to the  $V_{max}/K_m$  ratio, determined from radiodetection data acquired during a constant infusion of low concentrations of radiolabeled substrate (i.e.,  $[S] \ll K_m$ ) in isolated rat hearts where extraneuronal uptake into myocytes (uptake-2) was blocked pharmacologically.

Comparing the PET radiotracers HED and EPI, both possess relative high  $V_{\max}$  values, but HED has a much lower  $K_m$  value, leading to a  $V_{\max}/K_m$  ratio that is 5.4 times higher for HED than that of EPI.

In the phenethylguanidine series, comparing the positional isomers [ $^{11}\text{C}$ ]para-hydroxyphenethylguanidine (PHPG) and [ $^{11}\text{C}$ ]meta-hydroxyphenethylguanidine (MHPG),  $K_m$  values are similar while  $V_{\max}$  for MHPG is 2.4 times higher, leading to a ratio  $V_{\max}/K_m$  is 1.8 times higher for MHPG. Adding a  $\beta$ -hydroxyl group to MHPG to form (–)-N-[ $^{11}\text{C}$ ]guanyl-meta-octopamine (GMO) causes a 6-fold increase in  $K_m$  and a 30% decrease in  $V_{\max}$ , leading to a  $V_{\max}/K_m$  ratio ~9 times slower than for MHPG. Adding para-fluoro to MHPG to form [ $^{11}\text{C}$ ]4-fluoro-meta-hydroxyphenethylguanidine (4F-MHPG) does not significantly change  $V_{\max}$ , but  $K_m$  increases 5-fold, decreasing  $V_{\max}/K_m$  relative to MHPG. For the ortho-fluoro analog of MHPG, [ $^{11}\text{C}$ ]6-fluoro-meta-hydroxyphenethylguanidine (6F-MHPG),  $K_m$  is similarly increased ~5-fold, but  $V_{\max}$  is also reduced ~50%, causing  $V_{\max}/K_m$  to be only ~12% of the value for MHPG. Thus  $\beta$ -hydroxy- and aromatic ring fluoro-substitutions into the MHPG backbone had larger effects on  $K_m$  than on  $V_{\max}$ .

There were no significant correlations between the binding affinities ( $K_i$ ) and transport parameters ( $K_m$ ,  $V_{\max}$ ), or combinations of these constants, as measured using C6-hNET cells. This differs from a previous finding of a significant negative linear correlation between the ratio  $K_m/K_i$  and  $V_{\max}$  measured for a set of seven NET substrates performed with rat pheochromocytoma (PC12) cells [22]. The reasons for these differences are unknown, but again, they could be due to the lack of membrane-bound cofactors related to NET transport that are present in PC12 cells but lacking in the transfected C6-hNET cells. For example, interaction of NET with the protein syntaxin 1A, which is involved in the exocytotic release of norepinephrine from vesicles, has been shown to modulate NET activity. In one study, cleavage of the interaction between syntaxin 1A and NET in tissue and cell preparations expressing NET caused a 50%–75% reduction in norepinephrine transport activity [23]. PC12 cells contain large concentrations of syntaxin 1A [24] while this protein is absent in C6 glioma cells [25]. In addition to syntaxin 1A, several other proteins are known to interact with monoamine transporters and modulate their activity [26]. Further studies would be needed to determine if missing membrane cofactors are the root cause of the different results between our data set and those previously reported for PC12 cells, or if a particular experimental condition, such as the use of reserpine to block vesicular monoamine transporters (VMAT) in PC12 cells [22], is involved. Nevertheless, a strong linear correlation ( $r^2 = 0.96$ ) was observed between NET-transport mediated neuronal uptake rates in isolated rat hearts ( $K_{up}$ ; ml/min/g wet) and the  $V_{\max}/K_m$  ratios determined in C6-hNET cells (Fig. 3). Since the  $K_{up}$  values measured in isolated rat hearts are for intact NET transporters in their native sympathetic nerve membranes, the high linear correlation with the  $V_{\max}/K_m$  ratios determined in vitro suggests that the C6-hNET cell studies provided accurate estimates of the transport parameters  $K_m$  and  $V_{\max}$  for hNET transport. Thus the relative magnitudes of the measured  $V_{\max}/K_m$  ratios likely reflect the relative rates at which the biogenic amines and PET radiopharmaceuticals tested in this study are transported by hNET into sympathetic neurons in the human heart.

## 5. Conclusion

In conclusion, the binding affinities ( $K_i$ ) and Michaelis–Menten transport constants ( $K_m$ ,  $V_{\max}$ ) of several radiolabeled NET substrates were measured using a cell line stably transfected with the cloned human NET. The results allow for a detailed comparison of the kinetic profiles of several key biogenic amines and some existing PET radiopharmaceuticals for imaging cardiac sympathetic innervation. In addition, the results show that this approach yields valuable structure–activity data, providing insights on how specific structural

changes influence NET binding affinity and transport constants. An important application of in vitro measurements of transport kinetic parameters will be to screen new sympathetic nerve imaging agents for a desired kinetic profile (especially the  $V_{\max}/K_m$  ratio) prior to biological testing in animal models. These studies will also contribute to the rational design of a novel tracer with more optimal in vivo kinetics for quantifying regional sympathetic nerve density with PET.

## Acknowledgments

We thank the staff of the University of Michigan Cyclotron Facility, especially Lou Tluczek for preparing [ $^{11}\text{C}$ ](–)-meta-hydroxyephedrine and [ $^{11}\text{C}$ ](–)-epinephrine. This work was supported by PHS grant R01-HL079540 from the National Heart Lung and Blood Institute, National Institutes of Health, Bethesda, MD USA.

## References

- [1] Bengel FM. Imaging targets of the sympathetic nervous system of the heart: translational considerations. *J Nucl Med* 2011;52:1167–70.
- [2] DeGrado TR, Hutchins GD, Toorongian SA, Wieland DM, Schwaiger M. Myocardial kinetics of carbon-11-meta-hydroxyephedrine: retention mechanisms and effects of norepinephrine. *J Nucl Med* 1993;34:1287–93.
- [3] Nguyen NTB, DeGrado TR, Chakraborty P, Wieland DM, Schwaiger M. Myocardial kinetics of C-11 epinephrine in the isolated working rat heart. *J Nucl Med* 1997;38:780–5.
- [4] Raffel DM, Wieland DM. Assessment of cardiac sympathetic nerve integrity with positron emission tomography. *Nucl Med Biol* 2001;28:541–59.
- [5] Raffel DM, Jung YW, Gildersleeve DL, Sherman PS, Moskwa JJ, Tluczek LJ, et al. Radiolabeled phenethylguanidines: novel imaging agents for cardiac sympathetic neurons and adrenergic tumors. *J Med Chem* 2007;50:2078–88.
- [6] Rosenspire KC, Haka MS, Van Dort ME, Jewett DM, Gildersleeve DL, Schwaiger M, et al. Synthesis and preliminary evaluation of carbon-11-meta-hydroxyephedrine: a false transmitter agent for heart neuronal imaging. *J Nucl Med* 1990;31:1328–34.
- [7] Chakraborty PK, Gildersleeve DL, Jewett DM, Toorongian SA, Kilbourn MR, Schwaiger M, et al. High yield synthesis of high specific activity R(–)-[ $^{11}\text{C}$ ] epinephrine for routine PET studies in humans. *Nucl Med Biol* 1993;20:939–44.
- [8] Lowry OH, Rosebrough NJ, Farr AL, Randall RJ. Protein measurements with the folin phenol reagent. *J Biol Chem* 1951;193:265–75.
- [9] Raffel DM, Chen W. Binding of [ $^3\text{H}$ ]mazindol to cardiac norepinephrine transporters: kinetic and equilibrium studies. *Naunyn-Schmiedeberg's Arch Pharmacol* 2004;370:9–16.
- [10] Iversen LL. The uptake and storage of noradrenaline in sympathetic nerves. Cambridge: Cambridge University Press; 1967.
- [11] Hellmann G, Hertting G, Peskar B. Uptake kinetics and metabolism of 7-3H-dopamine in the isolated perfused rat heart. *Br J Pharmacol* 1971;41:256–69.
- [12] Iversen LL. The uptake of noradrenaline by the isolated perfused rat heart. *Brit J Pharmacol* 1963;21:523–37.
- [13] Iversen LL. The uptake of catechol amines at high perfusion concentrations in the rat isolated heart: a novel catechol amine uptake process. *Br J Pharmacol* 1965;25:18–33.
- [14] Iversen LL. Role of transmitter uptake mechanisms in synaptic neurotransmission. *Br J Pharmacol* 1971;41:571–91.
- [15] DeGrado TR, Zalutsky MR, Coleman RE, Vaidyanathan G. Effects of specific activity on meta-[ $^{131}\text{I}$ ]iodobenzylguanidine kinetics in isolated rat heart. *Nucl Med Biol* 1998;25:59–64.
- [16] Raffel D, Loc'h C, Mardon K, Mazière B, Syrota A. Kinetics of the norepinephrine analog [Br-76]-meta-bromobenzylguanidine in isolated working rat heart. *Nucl Med Biol* 1998;25:1–16.
- [17] Kim CH, Kim HS, Cubells JF, Kim KS. A previously undescribed intron and extensive 5' upstream sequence, but not Phox2a-mediated transactivation, are necessary for high level cell type-specific expression of the human norepinephrine transporter gene. *J Biol Chem* 1999;274:6507–18.
- [18] Eshleman AJ, Neve RL, Janowsky A, Neve KA. Characterization of a recombinant human dopamine transporter in multiple cell lines. *J Pharmacol Exp Ther* 1995;274:276–83.
- [19] Johnson RA, Eshleman AJ, Meyers T, Neve KA, Janowsky A. [ $^3\text{H}$ ]Substrate- and cell-specific effects of uptake inhibitors on human dopamine and serotonin transporter-mediated efflux. *Synapse* 1998;30:97–106.
- [20] Foley KF, Van Dort ME, Sievert MK, Ruoho AE, Cozzi NV. Stereospecific inhibition of monoamine uptake transporters by meta-hydroxyephedrine isomers. *J Neur Transm* 2002;109:1229–40.
- [21] Stein WD. Transport and diffusion across cell membranes. London: Academic Press; 1986.
- [22] Schömig E, Korber M, Bönisch H. Kinetic evidence for a common binding site for substrates and inhibitors of the neuronal noradrenaline carrier. *Naunyn-Schmiedeberg's Arch Pharmacol* 1988;337:626–32.
- [23] Sung U, Apparsundaram S, Galli A, Kahlig KM, Savchenko V, Schroeter S, et al. A regulated interaction of syntaxin 1A with the antidepressant-sensitive

- norepinephrine transporter establishes catecholamine clearance capacity. *J Neurosci* 2003;23:1697–709.
- [24] Bennett MK, Garcia-Ararras JE, Elferink LA, Peterson K, Fleming AM, Hazuka CD, et al. The syntaxin family of vesicular transport receptors. *Cell* 1993;74:863–73.
- [25] Fournier KM, Robinson MB. A dominant-negative variant of SNAP-23 decreases the cell surface expression of the neuronal glutamate transporter EAAC1 by slowing constitutive delivery. *Neurochem Int* 2006;48:596–603.
- [26] Sager JJ, Torres GE. Proteins interacting with monoamine transporters: current state and future challenges. *Biochemistry* 2011;50:7295–310.